PHYSICAL REVIEW E VOLUME 50, NUMBER 3 SEPTEMBER 1994

Flow-induced scattering peak in the structure factor of polymer solutions

Denis Wirtz
Chemical Engineering Department, The Johns Hopkins University, Baltimore, Maryland 21218
(Received 2 May 1994; revised manuscript received 13 July 1994)

We demonstrate that, at low shear rates, the scattering peak in the structure factor of sheared polymer solutions results from the combined effects of advection and flow-induced concentration fluctuation enhancement. Using time-resolved small angle light scattering, the distance of the peak from the origin of the reciprocal space is shown to scale as $\dot{\gamma}^{1/2}$, where $\dot{\gamma}$ is the shear rate of the flow.

PACS number(s): 61.25.Hq

A strong flow field can couple with the long-lived internal degrees of freedom of a fluid system and enhance the concentration fluctuations. This effect of flow-induced concentration fluctuation enhancement has recently motivated much research in complex fluids including lyotropic liquid crystals, swollen gels, and polymer fluids [1–9]. Light scattering experiments show that dramatic fluctuation enhancement is also produced when a semidilute polymer solution is subjected to an external uniform shear flow [5–8]. In this case, the light scattering patterns are characteristically distinguished by an intermediate broad peak. Helfand and Fredrickson (HF) [1] unraveled the mechanism of fluctuation enhancement in polymer solutions. Yet, the origin of the scattering peak remains poorly understood. Predicting the presence of this scattering peak is thus a crucial test for any dynamical theory that describes polymer solutions brought outside of equilibrium by an external flow field. The goal of this Rapid Communication is to demonstrate experimentally that the scattering peak results from combined effects of HF fluctuation enhancement and advection of the fluctuations.

The original HF dynamic model does not predict the existence of a scattering peak in the structure factor of sheared polymer solutions. Recently, Milner [3] added a phenomenological equation of motion for the fluid strain to the original HF dynamical equation for the concentration field. Milner's model predicts that the scattering peak is independent of shear rate, and corresponds to the crossover from a simple binary fluid to a transient gel network [10]. A major improvement of the HF model seen in Milner's theory is the prediction that light scattering is sharply reduced at large scattering angles, as is observed experimentally [5–8]. However, significant discrepancies between these models and our experimental observations remain. They include qualitative disagreement between measured and calculated positions and orientations of the scattering peak and scattering patterns with respect to the flow direction.

To compare our experimental findings to results previously published in the literature, we chose the widely used [5–8] semidilute solution of polystyrene in dioctyl phtalate (PS-DOP) for our polymer-solvent system. The molecular weight of the polymer is $M_w = 1\,850\,000$, with an index of polydispersity of $M_w/M_n = 1.06$ (M_n is the number-average molecular weight). The polymer concentration, $c = 6$ wt %, is larger than the semidilute crossover concentration. This polymer solution is sheared in a Couette flow cell composed of two concentric cylinders (gap width $= 0.36$ cm, optical path length $= 1$ cm), maintained at a constant temperature T ($\pm 0.1\,^\circ$C), between the cloud point temperature T_c and the θ temperature of the solution, $T_c = 11\,^\circ\text{C} < T = 16\,^\circ\text{C} < \theta = 22\,^\circ$C. T_c separates the one-phase region from the two-phase region of the polymer solution; θ is the temperature corresponding to the Flory compensation point [11] where the excluded volume interaction between polymer segments vanishes. The evolution of the scattering patterns is monitored by time-resolved small-angle light scattering (SALS) in the flow-shear plane, normal to the incident light of a He-Ne laser ($\lambda = 632.8$ nm). Images of the scattering patterns are acquired via a charge coupled device (CCD) camera and a frame grabber at a rate of up to 3 frames per second. The position of the scattering peak and the orientation of the patterns are computed using the SALS computer software developed by van Egmond, Werner, and Fuller [5]. Further details regarding the SALS setup, the flow cell, the image acquisition procedure, and the polymer-solvent system can be found in Refs. [5,12].

Figure 1 displays steady state scattering patterns both for a quiescent PS-DOP solution and for the same solution subjected to two increasing (low) shear rates. These scattering patterns are isointensity contours of light scattered by the sheared polymer solution. In the absence of flow, light scattering is isotropic; in the presence of a shear flow, light scattering is anisotropically enhanced. The corresponding flow-induced enhancement of the concentration fluctuations is due to an effective coupling between the polymer concentration field and the fluctuating viscoelastic stress via concentration-dependent transport coefficients (shear viscosity, normal stress coefficients, elasticity constants [1,2]. Further, Fig. 1 reveals that, in the reciprocal Fourier space, the distance of the peak from the q-space origin is *increased* from $q = 0$ in the absence of shear, to an intermediate distance $q = q_{\text{peak}}(\dot{\gamma}\tau)$ for increasing rates of shear. These experimental observations contradict Milner's model. Indeed, Milner's model predicts that, even in the presence of shear, the peak remains at a *fixed* "magic length" [2,3,10] given by $\lambda_{\text{peak}} = 2\pi/q_{\text{peak}} = 2\pi(\tau D)^{1/2}$. D is the mutual diffusion coefficient and τ is the stress relaxation time of the polymer. Both constants were measured by van Egmond, Werner, and Fuller [5] at $T = 16$ °C: $D = 0.02$ μm^2/s and $\tau = 0.995$ s, which yields the fixed distance $q_{\text{peak}} \cong 7.1$ μm^{-1}. As shown in Fig. 1, this value does not agree with our peak position measurements.

 © 1994 The American Physical Society

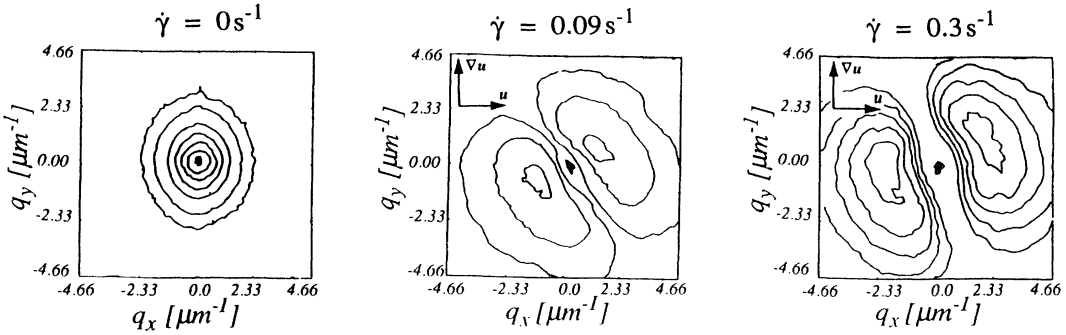

FIG. 1. Measured light scattering patterns in the flow-shear plane in the absence of flow and for two increasing shear rates. The scattering patterns rotate towards the flow direction and the distance of the scattering peak from the q-space origin increases with increasing shear rates (at low shear rates).

Figure 2 displays the measured distance of the scattering peak from the origin of the Fourier space as a function of shear rate. Two types of measurements of the scattering peak position are feasible. The scattering peak is given either by the point where maximum scattering occurs in the plane normal to the incident light, $q_{\text{peak}}=q_{\text{peak}}^{\text{max}}$, or is computed by scattering average, $q_{\text{peak}}=q_{\text{peak}}^{\text{av}}$:

$$q_{\text{peak}}^{\text{max}}=q|_{I(\mathbf{q})\text{max}}$$

or (1)

$$q_{\text{peak}}^{\text{av}}=\left(\frac{\int d\mathbf{q}\, q^2[I(\mathbf{q})-I_0(q)]\delta(\phi_s-\phi(\mathbf{q}))}{\int d\mathbf{q}[I(\mathbf{q})-I_0(q)]\delta(\phi_s-\phi(\mathbf{q}))}\right)^{1/2}.$$

$I_0(q)$ is the scattering intensity in the absence of flow, ϕ_s is the angle of orientation of the major axis of the scattering pattern with respect to the flow direction, and $\phi(\mathbf{q})$ is the azimuthal angle in the plane normal to the incident light. Figure 2 shows that the distance of the scattering peak from the q-space origin is increased for augmenting (but small) shear rates. Both types of peak position measurements confirm this important result. Therefore one can assert that current models [1–4] are unable to reproduce scattering experiments even in the low shear rate regime.

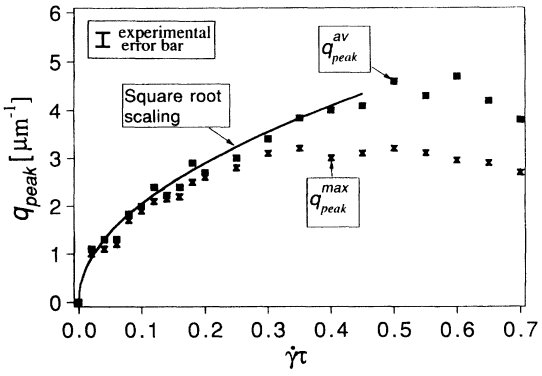

FIG. 2. Distance of the scattering peak from the q-space origin as a function of shear rate. The position of the peak is measured by scattering average ($q_{\text{peak}}^{\text{av}}$) and by maximum intensity detection ($q_{\text{peak}}^{\text{max}}$). The curve in bold corresponds to a square root fit of the data.

We now show that, at low shear rates and at low scattering angles, the presence of a scattering peak in the structure factor can be explained by the HF model as long as advection is added to the original HF description. The measured steady state SALS intensity $I(\mathbf{q})$ is proportional to the structure factor $S(\mathbf{q})$, which is the Fourier transform of the equal-time correlation function of the concentration fluctuations. The original HF equation of motion for $S(\mathbf{q})$ [Eq. (10) in Ref. [2]] in a uniform shear flow $\mathbf{u}=\dot{\gamma}y\mathbf{e}_x$ can be rewritten

$$\left[2\xi^2q^2S_{\text{HF}}^{-1}(\mathbf{q})-\text{Pe}q_x\frac{\partial}{\partial q_y}\right]S(\mathbf{q})=2\xi^2q^2. \quad (2)$$

The first term in this equation describes HF flow-induced fluctuation enhancement, where ξ is the quiescent correlation length and $S_{\text{HF}}(\mathbf{q})$ is the steady state HF structure factor in the absence of advection given by Eq. (13) in Ref. [2]. The second term describes the advection of the fluctuations, where $\text{Pe}=\dot{\gamma}\xi^2/D$ is the Péclet number. This number compares the relative strengths of advection and diffusion effects in the transport of the concentration fluctuations under shear, with $\dot{\gamma}$ the shear rate. In Eq. (2), q_i denotes the Cartesian coordinates of the scattering vector $\mathbf{q}$. The term on the right-hand-side of Eq. (2) is thermal noise and is assumed to possess Gaussian statistics. In the absence of advection [see Figs. 3(a) and 3(c)], the structure factor $S(\mathbf{q},\text{Pe}=0)$ assumes the HF form $S_{\text{HF}}(\mathbf{q})$. In this case, the scattering peak is located at the origin of the q space, with a discontinuity at $q=0$. Figures 3(b) and 3(c) display the structure factor $S(\mathbf{q},\text{Pe}\neq 0)$ when advection is included, obtained by numerical solution of Eq. (2). Figure 3 demonstrates that advection suppresses the small-q long-lived fluctuations, enhances the scattering intensity, and further rotates scattering patterns in the flow direction, even for very small values of Pe. As a result, a scattering peak appears at an intermediate q value. According to Eq. (2), this new scattering intensity peak corresponds to the point where diffusion and advection effects cancel. Hence the peak is the locus of points in q space given by $2q^2\xi^2S_{\text{HF}}^{-1}(\mathbf{q})\cong\text{Pe}q_x/q_y$. This last equality predicts that the distance of the peak from the q-space origin scales as $q_{\text{peak}}\sim\xi^{-1}\text{Pe}^{1/2}(1-\dot{\gamma}\tau\partial\eta/\partial\varphi)^{-1/2}$ for $\dot{\gamma}\tau\ll 1$. Here, φ and η are the polymer volume fraction and the (dimensionless) viscosity of the polymer solution, respectively [1]. Figure 2 shows that indeed $q_{\text{peak}}\sim\dot{\gamma}^{1/2}$ at low shear rates [13], which

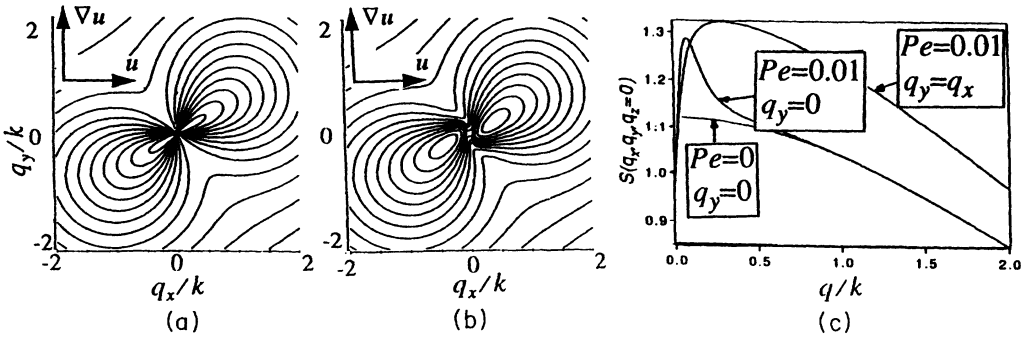

FIG. 3. Calculated isointensity contours and scattering profiles of the steady state structure factor in the flow-shear plane: (a) without advection, Pe=0; (b) with advection, Pe=0.01; (c) $S(q_x,q_y,q_z=0)$ vs q with and without advection. $\dot{\gamma}\tau=0.34$, $k\xi=0.26$, $\partial\eta/\partial\varphi=0.66$, $\partial\Psi_1/\partial\varphi=1.31$, $\partial\Psi_2/\partial\varphi=-0.4$ [8,1]. The structure factors are scaled by $S(\mathbf{q}=\mathbf{0})$; k is the wave vector of the probing light, Ψ_1 and Ψ_2 are the first and second normal stress coefficients of the polymer solution [1].

confirms that advection is responsible for the transport of the peak from the origin. However, the distance q_{peak} reaches a maximum value when the shear rate attains a threshold value $\dot{\gamma}=0.4\ \text{s}^{-1}$ and decreases for shear rates $\dot{\gamma}\geq 0.4\ \text{s}^{-1}$. This effect cannot be explained by the above linear theory. In addition, as pointed out by Milner [3], the HF model on which Eq. (2) is based is oversimplified since the scattering intensity at large scattering angles is not only decreased by the term $q\xi$ in Eq. (2), but also by the important dynamics of polymer elastic strain at large q. It is important to note that numerical integration of the coupled equations of motion for the concentration field and the polymer strain (see Fig. 3, Ref. [3]) does show both the onset of the scattering peak and the displacement of the peak from the origin for increasing shear rates when advection is included. Yet, even when an equation for the polymer strain is added to the HF model, calculated scattering patterns do not possess an intermediate peak in the absence of advection (see Fig. 5, Ref. [3]).

We analyze next the orientation of the scattering patterns in the flow-shear plane. The steady state scattering angle of the major axis of the scattering patterns with respect to the flow direction is evaluated by

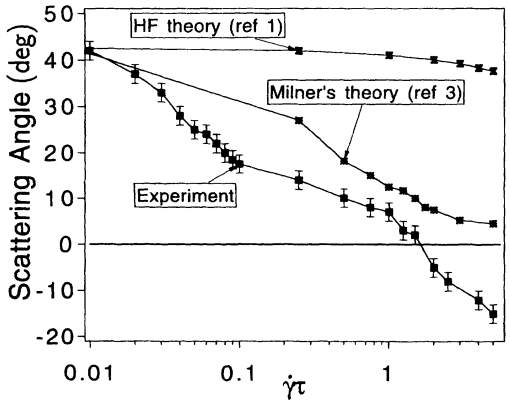

FIG. 4. Measured and calculated orientation angles of the scattering peak with respect to the flow direction as a function of shear rate. The pattern orientation angle becomes negative for $\dot{\gamma}\tau\geq 1.85$.

$$\tan 2\phi_s=\frac{2\langle q_xq_y\rangle}{\langle q_xq_x\rangle-\langle q_yq_y\rangle}, \tag{3}$$

where $\langle q_iq_j\rangle=\int d\mathbf{q}\,I(\mathbf{q})q_iq_j/\int d\mathbf{q}\,I(\mathbf{q})$. Figure 4 displays both the orientation angle of the major axis with respect to strain rate measured by SALS using Eq. (3) and the orientation angle calculated using both HF and Milner's models [1,3]. At vanishing shear rates, patterns are oriented at 45° with respect to the flow direction; the patterns rotate towards the flow direction for increasing shear rates. No *quantitative* agreement between measured and calculated pattern orientation angles is obtained at low shear rates: The calculated angle always exceeds the measured angle. Furthermore, no *qualitative* agreement is observed at large shear rates since measured pattern orientation angles become negative for $\dot{\gamma}\tau\geq 1.85$, unlike calculated pattern orientation angles which are always positive. The rotation of the patterns towards the flow direction for increased shear rates is usually explained by normal stress effects [1–4]. Advection accentuates ensemble rotation of the scattering patterns towards the flow direction, as shown in Fig. 3. However, current theories are unable to explain the mechanism by which the patterns rotate beyond the flow axis at high shear rates as shown in Fig. 4. Finally, upon the cessation of flow and for large shear rates, a strong scattering overshoot occurs, whose intensity increases with shear rate. This nonlinear viscoelastic effect cannot be predicted because current analytical theories employ simple linear constitutive equations to describe the polymer stress. In conclusion, theoretical advancement is necessary to explain our measurements of both position and orientation of the scattering peak present in the structure factor of sheared polymer solutions.

This work was conducted in the rheo-optics laboratory at Stanford University. Valuable experimental help from J. Lai and D. E. Werner is gratefully acknowledged. The author would like to express his gratitude to J. Harden, R. Bruinsma, and D. J. Pine for fruitful comments. This research was partially supported by the EU.

[1] E. Helfand and G. H. Fredrickson, Phys. Rev. Lett. **62**, 2468 (1989).
[2] S. T. Milner, Phys. Rev. Lett. **66**, 1477 (1991).
[3] S. T. Milner, Phys. Rev. E **48**, 3674 (1993).
[4] A. Onuki, Phys. Rev. Lett. **62**, 2472 (1989).
[5] J. W. van Egmond, D. E. Werner, and G. G. Fuller, J. Chem. Phys. **96**, 7742 (1992).
[6] H. Hashimoto, T. Takebe, and S. Suehiro, J. Chem. Phys. **88**, 5874 (1988).
[7] X.-l. Wu, D. J. Pine, and P. K. Dixon, Phys. Rev. Lett. **62**, 2408 (1991).
[8] P. K. Dixon, D. J. Pine, and X.-l. Wu, Phys. Rev. Lett. **66**, 2239 (1992).
[9] R. Bruinsma and C. R. Safinya, Phys. Rev. A **43**, 5377 (1991); R. Bruinsma and Y. Rabin, *ibid.* **45**, 994 (1992); R. Bruinsma and Y. Rabin, Phys. Rev. E **49**, 554 (1994).
[10] F. Brochard and P.-G. de Gennes, Macromolecules **10**, 1157 (1977).
[11] P. Flory, *Principles of Polymer Chemistry* (Cornell University Press, Ithaca, NY, 1971).
[12] D. Wirtz, K. Berend, and G. G. Fuller, Macromolecules **25**, 7234 (1992); D. Wirtz and G. G. Fuller, Phys. Rev. Lett. **71**, 2236 (1993); D. Wirtz, D. E. Werner, and G. G Fuller, J. Chem. Phys. **101**, 1679 (1994).
[13] Similar $q_{\text{peak}} \sim \dot{\gamma}^{1/2}$ scaling was found by S. Ramaswamy, Phys. Rev. A **29**, 1506 (1984) and O. Diat, D. Roux, and F. Nallet, J. Phys. (France) II **3**, 1427 (1993).